PHYSICAL REVIEW B VOLUME 45, NUMBER 11 15 MARCH 1992-I

Observation of electronic subbands in dense arrays of quantum wires grown by organometallic-chemical-vapor deposition on nonplanar substrates

M. Walther, E. Kapon, D. M. Hwang, E. Colas, and L. Nunes*
Bellcore, Red Bank, New Jersey 07701
(Received 13 December 1991)

We report luminescence and absorption properties of dense arrays of narrow (14 nm), crescent-shaped GaAs/$Al_xGa_{1-x}As$ quantum wires (QWRs) grown by organometallic-chemical-vapor deposition on nonplanar substrates. Low-temperature photoluminescence (PL) spectra of the samples are dominated by emission from the QWRs, indicating efficient carrier transfer into the wires from the surrounding quantum wells and barriers. PL excitation spectra of the wires exhibit enhanced absorption at the electron–heavy-hole subbands with a measured subband separation of 34–39 meV, in good agreement with calculated values. Achievement of such large subband separations, on the order of k_BT at room temperature (for electrons), is important for investigations of quasi-one-dimensional systems in which only the ground state of the QWR is populated.

Low-dimensional semiconductor heterostructures have attracted increasing interest in recent years because of their novel properties and potential device applications.[1–3] Our approach for preparing quantum wires (QWRs) and dots by epitaxial growth on nonplanar substrates[4] allows *in situ* formation of their interfaces, thus avoiding interface damage introduced by the more conventional etching and regrowth techniques.[5,6] This is particularly important for optical studies, since interface damage can severely reduce carrier lifetime and degrade quantum efficiency. Crescent-shaped QWRs grown by organometallic-chemical-vapor deposition (OMCVD) on V-grooved substrates exhibit efficient luminescence and radiative carrier lifetimes comparable to that of conventional quantum well (QWL) heterostructures.[7–9] Furthermore, QWR lasers incorporating such wires oscillate at room temperature with sub-mA threshold currents[10] and their spectra show evidence for two-dimensional (2D) quantum confinement.[7,11] However, these studies have been limited so far to QWR structures with relatively small electronic subband separation (less than k_BT at room temperature) and to QWR arrays of relatively low density (several μm pitch). Increasing the energy separation between the subbands is important for achieving quasi-1D carriers which populate predominantly the QWR ground state. Decreasing the wire spacing to less than the carrier diffusion length allows carrier thermalization into the wires, thus avoiding competing recombination and trapping in the wire barriers. Both effects will be useful for improving the performance of optical and electronic devices relying on QWR structures.

In the present paper we discuss the optical properties of arrays of GaAs/$Al_xGa_{1-x}As$ QWRs of 240 nm pitch and only 14 nm effective width. In contrast to arrays with pitch greater than the carrier diffusion length,[8,9] photoluminescence (PL) spectra of these structures are dominated by recombination in the QWRs due to lateral carrier thermalization from the surrounding QWLs into the lower-energy QWR. PL excitation spectra clearly show the first two electron–heavy-hole QWR transitions with 34–39 meV (total) subband separation. The measured subband separations are in good agreement with model calculations based on transmission electron microscopy (TEM) cross sections of the wires. The electron subband separation in these structures are of the order of k_BT at room temperature.

Figure 1 shows TEM cross-sectional images of the QWR structure discussed here. The structure was prepared by first patterning a (100) semi-insulating GaAs substrate with periodic corrugations of 240 nm pitch and 120 nm depth using holographic photolithography and wet chemical etching. The grating grooves were oriented along the $[01\bar{1}]$ direction. Atmospheric-pressure OMCVD was then used to grow a 150-nm-thick $Al_{0.5}Ga_{0.5}As$ lower cladding layer, followed by 1-nm-thick GaAs QWL layer and 30-nm-thick upper $Al_{0.5}Ga_{0.5}As$ cladding layer. All layers were nominally undoped and thicknesses correspond to growth rates on planar surfaces (for more details on the growth procedures see Ref. 12).

Growth on the patterned substrate results in formation of 2.8-nm-thick, crescent-shaped GaAs wires interconnected by much thinner ($\sim$1 nm) GaAs QWL regions. The wires are formed due to enhanced migration of Ga species to the bottom of the grooves during the OMCVD growth step.[7,8] Additionally, this migration leads to formation of a Ga enriched vertical stripe in the $Al_xGa_{1-x}As$ above and below the QWR crescent (see vertical dark stripes in Fig. 1). The lateral tapering of the QWL at the crescent gives rise to a lateral potential well that defines the QWR. This is illustrated in Fig. 2, which describes a model of the 2D quantum confinement in these wires. The lateral thickness distribution of the QWL crescent was measured from the TEM cross sections. The resulting lateral potential wells for each carrier type were then evaluated by calculating the confinement energies E_{conf} for each thickness using a finite-well model in the effective-mass approximation.[13] The lateral potential wells were fitted with $1/\cosh^2$ profiles which allow analytical solution of the eigenenergies and wave functions for the QWR subbands.[7] The total (i.e., transverse plus lateral) confinement energies for the four lowest QWR states are summarized in Table I. The energy levels of the

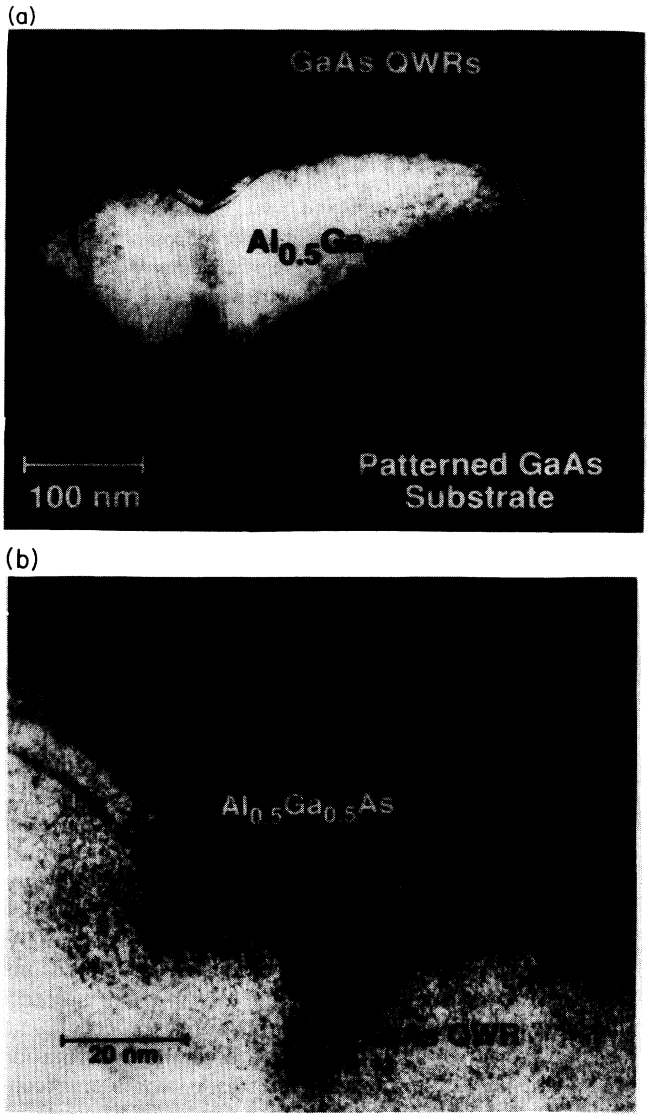

FIG. 1. (a) Transmission electron microscope cross section of the quantum wire array. (b)Magnified view of a crescent-shaped wire.

electron subbands are also indicated by the horizontal lines in Fig. 2. A measure of the effective width W_{eff} of these tapered QWR structures is given by the lateral separation between the points at which the lateral wave functions become exponentially decaying. For electrons in the ground state, we calculated $W_{\text{eff}}=14$ nm, which is considerably narrower than the geometrical width of the wire.

Figure 3 shows the PL spectrum of the sample at $T=5$ K. The spectrum is dominated at low temperatures by luminescence from the QWR emitted at 1.76 eV. In contrast to previous studies of arrays of crescent-shaped QWRs with μm size pitch,[9,14] we observe only very weak luminescence from the surrounding QWL layers, even at low temperatures. This is well explained by the fact that the QWL sections connecting the wires are much shorter compared to the carrier diffusion length. Thus, all carriers absorbed in the QWL are collected in the low-energy QWRs before they can recombine in the QWL layers.

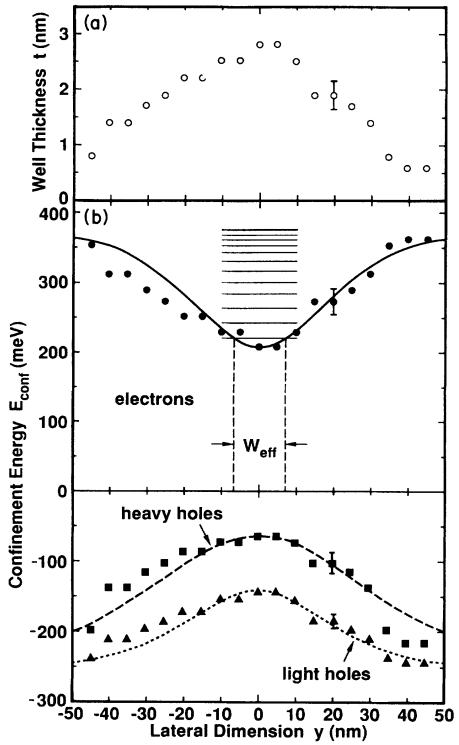

FIG. 2. Model of the quantum wire shown in Fig. 1(b). (a) Lateral thickness distribution of the quantum well at the crescent. (b) Lateral distribution of confinement energy E_{conf} for electrons, heavy holes, and light holes, calculated from part (a) (circles, squares, and triangles, respectively). Lines are $1/\cosh^2$ fits of the lateral potential wells. Horizontal bars represent the quantum wire subbands for electrons.

Measurements of the recombination dynamics[15] yield sub-ps carrier capture times and carrier lifetime of 0.3 ns.

Photoluminescence excitation (PLE) spectra of the QWR sample, detected at 696 nm (1.782 eV), are displayed in Fig. 4. The spectra were measured using a tunable DCM-dye laser, with the pump beam polarized parallel ($\parallel$) and perpendicular ($\perp$) to the wire axis. The strong increase in the PLE signal at $\sim$1.96 eV is due to absorption in the thin QWL layers between the wires, and possibly also in the vertical (Ga-enriched) $Al_xGa_{1-x}As$ stripes above and below the wires. Carriers captured in these regions subsequently diffuse and thermalize at the deeper potential well of the QWR, where they recombine radiatively. The smaller peaks near 1.8 eV are due to absorption at the QWR subbands. The ratio of 1:10 between the QWR and QWL absorption peaks is consistent with the ratio of the corresponding areas, implying com-

TABLE I. Confinement energies (meV) for electrons, and heavy and light holes for the QWR crescent of Fig. 1.

Subband index l	1	2	3	4
Electrons	219.6	242.6	263.8	283.1
Heavy holes	66.5	73.2	79.8	86.3
Light holes	151.1	166.7	180.9	193.8

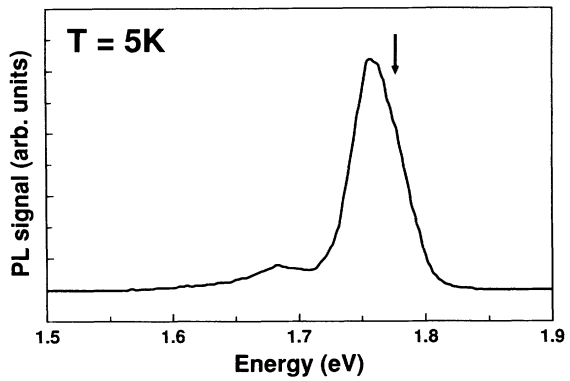

FIG. 3. Photoluminescence spectrum of the quantum wire array, excited with an argon-ion laser. Arrow indicates detection energy of the spectra in Fig. 4.

parable absorption coefficients for the wires and wells.

Two absorption peaks are clearly observable in the PLE spectra at 1.80 and 1.84 eV. Their positions are determined more accurately from the second derivative of the PLE spectra (dashed lines in Fig. 4), obtained using a spline approximation. The second derivatives of the spectra also reveal two additional absorption peaks at higher energies. The calculated transition energies corresponding to electron–heavy-hole and electron–light-hole transitions, derived from Table I assuming $E_g(\mathrm{GaAs}) = 1.519$ eV (neglecting excitonic effects), are indicated by the arrows in Fig. 4. Good agreement is obtained for the positions of the two lowest-lying QWR states. The lower (by ~ 10 meV) measured energy of the ground state compared to the calculated value may be due to excitonic effects. The Stokes shift of ~ 40 meV is consistent with the relatively broad luminescence line (46-meV full width at half maximum). This line broadening is attributed to thickness as well as alloy composition fluctuations in these very thin and narrow wires. Note that the lowest-lying electron–light-hole QWR transition energy is well separated from those of the lowest-energy electron–heavy-hole ones. Therefore, we expect little mixing between valence band levels originating from the lowest-lying light- and heavy-hole states,[16] and thus better agreement with our simple model which does not account for such mixing. Comparison of the two polarized spectra in Fig. 4 reveals only small anisotropy in the absorption features. This is consistent with the fact that our crescent-shaped wires have asymmetric cross sections (i.e., thickness much smaller than width), which should greatly reduce anisotropy effects.[16,17] However, it should be noted that electromagnetic grating effects might also introduce polarization anisotropy, which should be properly accounted for when interpreting the data.

In summary, we have reported luminescence and

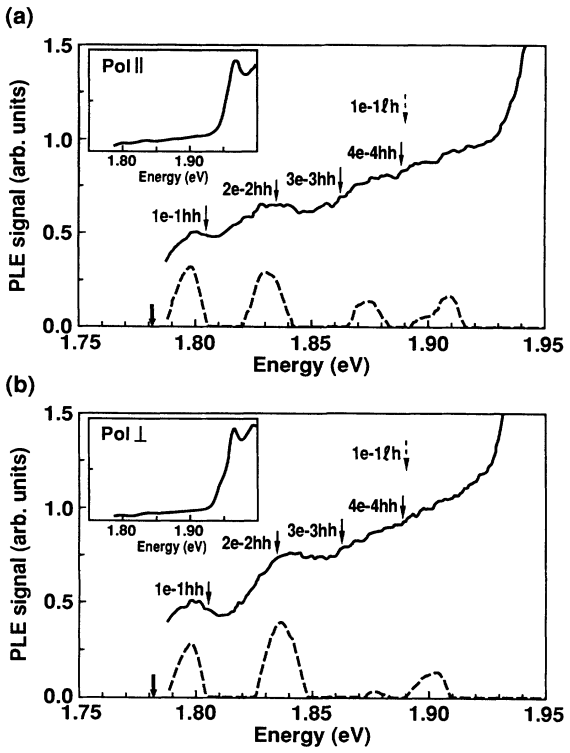

FIG. 4. Photoluminescence excitation spectra (solid lines) of the quantum wire array and their second derivative (dashed lines), measured at 5 K. Data are shown for pump beam polarizations (a) parallel and (b) perpendicular to the wires. Heavy arrow shows detection energy. Light arrows indicate energy positions of the calculated electron–heavy-hole (e-hh) and electron–light-hole (e-lh) quantum wire transition energies. Insets display the entire measured spectra, showing absorption at the quantum wells connecting the quantum wires.

absorption properties of dense arrays of 14-nm-wide, $\mathrm{GaAs/Al}_x\mathrm{Ga}_{1-x}\mathrm{As}$ QWRs grown on nonplanar substrates. Carrier thermalization from the surrounding QWL and barrier material into the wires and high-quality wire interfaces result in efficient luminescence from these wires. PLE spectra of the QWRs exhibit transitions between electron and heavy-hole QWR levels, with measured energy separation of 34–39 meV, in good agreement with model calculations. The lowest QWR electron subbands are separated by 23 meV, on the order of k_BT at room temperature. Such large subband separations are important for minimizing the thermal population of higher-level subbands, which is essential for room-temperature applications of these quantum structures.

We thank S. Simhony for help with grating fabrication and C. Chen for assistance with electron microscopy.

*Present address: Instituto de Fisica de São Carlos, Universidade de São Paulo, 13 560 São Paulo, São Paulo, Brazil.

[1]S. Schmitt-Rink, D. S. Chemla, and D. A. B. Miller, Adv. Phys. **38**, 89 (1989).

[2]K. Kash, J. Lumin. **46**, 69 (1990).

[3]Y. Arakawa and A. Yariv, IEEE J. Quantum Electron. **22**, 1887 (1986).

[4]E. Kapon, M. C. Tamargo, and D. M. Hwang, Appl. Phys.

Lett. **50**, 347 (1987).

[5]E. M. Clausen, Jr., H. G. Craighead, J. M. Worlock, J. P. Harbison, L. M. Schiavone, L. Florez, and B. P. van der Gaag, Appl. Phys. Lett. **55**, 1427 (1989).

[6]G. Mayer, B. E. Maile, R. Germann, A. Forchel, P. Grambow, and H. P. Meier, Appl. Phys. Lett. **56**, 2016 (1990).

[7]E. Kapon, D. M. Hwang, and R. Bhat, Phys. Rev. Lett. **63**, 430 (1989).

[8]E. Kapon, J. Christen, E. Colas, R. Bhat, D. M. Hwang, and L. M. Schiavone, in *Proceedings of the International Symposium on Nanostructures and Mesoscopic Systems, Sante Fe, NM, 1991*, edited by W. Kirk (Academic, New York, in press).

[9]J. Christen, E. Kapon, E. Colas, D. M. Hwang, L. M. Schiavone, M. Grundmann, and D. Bimberg, Surf. Sci. (to be published).

[10]S. Simhony, E. Kapon, E. Colas, D. M. Hwang, N. G. Stoffel, and P. Worland, Appl. Phys. Lett. **59**, 2225 (1991).

[11]E. Kapon, D. M. Hwang, M. Walther, R. Bhat, and N. G. Stoffel, Surf. Sci. (to be published).

[12]E. Colas, S. Simhony, E. Kapon, R. Bhat, D. M. Hwang, and P. S. D. Lin, Appl. Phys. Lett. **57**, 914 (1990).

[13]We use 0.6 conduction-band offset to band-gap ratio and $m_e = 0.0665 + 0.0735x$, $m_{hh} = 0.377 + 0.253x$, and $m_{lh} = 0.092 + 0.1x$ for effective masses in $Al_xGa_{1-x}As$; see H. Hilmer, A. Forchel, S. Hansmann, M. Morohashi, and E. Lopez, Phys. Rev. B **39**, 10901 (1989). Our model neglects anisotropy in hole masses; however, since the relative contribution of the heavy holes to total confinement energy is small, we expect fair agreement with measured subband separation, as indeed is the case.

[14]M. Walther, E. Kapon, J. Christen, D. M. Hwang, and R. Bhat, Appl. Phys. Lett. **60**, 521 (1992).

[15]J. Christen, M. Grundmann, E. Kapon, E. Colas, D. M. Hwang, L. M. Schiavone, and D. Bimberg (unpublished).

[16]U. Bockelmann and G. Bastard, Europhys. Lett. **15**, 215 (1991).

[17]M. Asada, Y. Miyamoto, and Y. Suematsu, Jpn. J. Appl. Phys. **24**, L95 (1985).

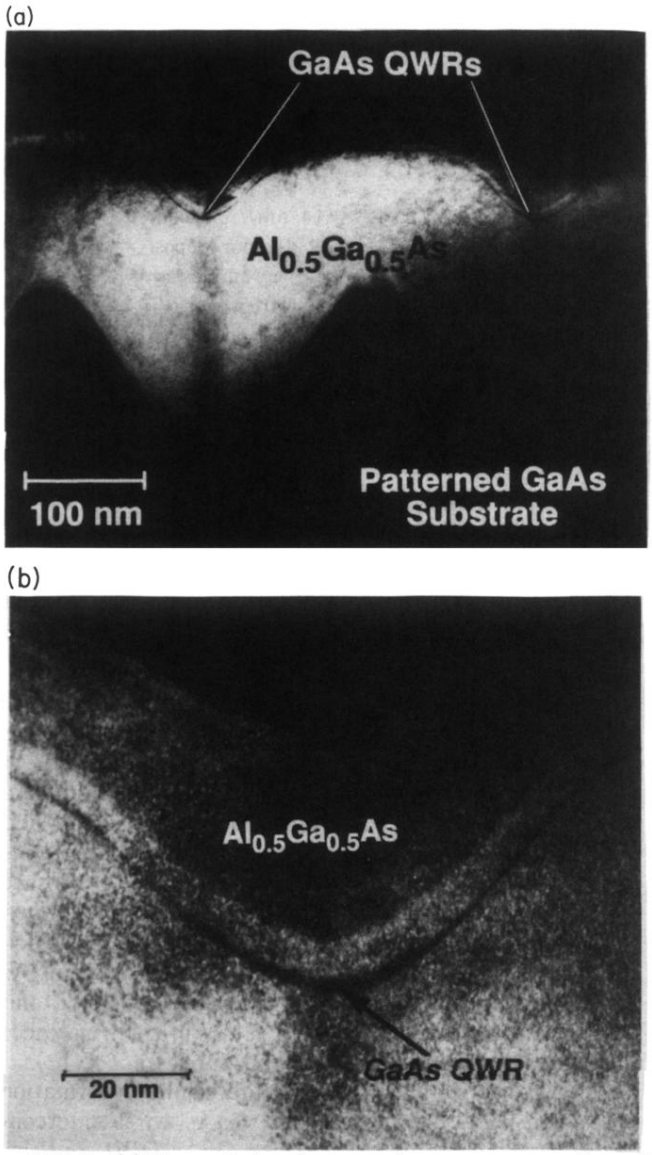

FIG. 1. (a) Transmission electron microscope cross section of the quantum wire array. (b)Magnified view of a crescent-shaped wire.